ACCSCIENCE PUBLISHING

Materials Science in Additive Manufacturing

ORIGINAL RESEARCH ARTICLE

Effects of heat treatment temperature and time on the fitness accuracy, retentive force, and permanent deformation of selective laser melting Ti-6Al-4V clasps

Lu-Xiang Yu[1,2†], Na Yu[1,2†], Jing-Jing Fan[1,2], Peng Wang[3], Lu Liu[3], and Fa-Bing Tan[1,2,4*]

[1]Department of Prosthodontics, College of Stomatology, Chongqing Medical University, Chongqing, China

[2]Chongqing Municipal Key Laboratory of Oral Biomedical Engineering of Higher Education, Chongqing Medical University, Chongqing, China

[3]Chongqing Jingmei Medical Technology Co., Ltd., Chongqing, China

[4]Chongqing Key Laboratory of Oral Diseases and Biomedical Sciences, Chongqing Medical University, Chongqing, China

[†]These authors contributed equally to this work.

***Corresponding author:**
Fa-Bing Tan
(xiaosongtan1983@hospital.cqmu.edu.cn)

Citation: Yu LX, Yu N, Fan JJ, Wang P, Liu L, Tan FB. Effects of heat treatment temperature and time on the fitness accuracy, retentive force, and permanent deformation of selective laser melting Ti-6Al-4V clasps. *Mater Sci Add Manuf.* 2026;5(2):025490118. doi: 10.36922/MSAM025490118

Received: December 7, 2025

1st revised: January 7, 2026

2nd revised: January 17, 2026

Accepted: January 20, 2026

Published Online: March 12, 2026

Copyright: © 2026 Author(s). This is an Open-Access article distributed under the terms of the Creative Commons Attribution License, permitting distribution, and reproduction in any medium, provided the original work is properly cited.

Publisher's Note: AccScience Publishing remains neutral with regard to jurisdictional claims in published maps and institutional affiliations.

Abstract

The selective laser melting (SLM) technology of Ti-6Al-4V (TC4) demonstrates significant advantages in fabricating clasps for removable partial dentures, whereas subsequent heat treatment plays a crucial role in performance optimization. This study systematically investigated the effects of heat treatment temperature and time on the fitness accuracy, retentive force, and permanent deformation of SLM TC4 clasps. TC4 clasp specimens were manufactured using SLM technology and subjected to heat treatment under different temperatures (700, 750, 800, and 850℃) and times (0.5, 1.0, and 1.5 h). The fitness accuracy, retentive force, and permanent deformation after 10,000 insertion/removal cycles were measured for each group and statistically analyzed. The results revealed that the 700℃/0.5 h group showed significantly reduced fitness accuracy. After cyclic testing, the retentive force of all groups decreased by 4.06%–12.18%, with heat treatment temperature significantly affecting both initial and final retentive forces. The time of heat treatment demonstrated no substantial influence. The permanent deformation of the clasps (31.15–38.05 μm) remained unaffected by variations in either heat treatment temperature or time. Based on overall performance, the 700℃/0.5 h heat treatment condition is not recommended. Instead, selecting shorter time protocols such as 0.5 h within the 750℃–850℃ range can help enhance production efficiency while maintaining performance standards.

Keywords: Heat treatment; Ti-6Al-4V clasp; Selective laser melting; Fitness accuracy; Retentive force; Permanent deformation

1. Introduction

Removable partial dentures (RPDs) remain essential in prosthodontic rehabilitation due to their broad indications, shorter treatment times, and relatively low cost.[1,2] Titanium and its alloys are extensively employed in RPD frameworks due to their excellent mechanical strength, corrosion resistance, and biocompatibility.[3] Over the years, traditional casting technology, as an equal-material manufacturing process, has been extensively applied and rigorously validated in the dental field.[4] Compared with computer numerical control machining, this method offers significant advantages, including high material utilization, low processing costs, and high production efficiency.[5] However, due to the exceptionally high melting point of titanium and its alloys, coupled with their high susceptibility to oxidation during melting, the fabrication of RPD titanium frameworks via casting continues to present substantial technical challenges, such as casting failure, incomplete mold filling, and excessive porosity.[6-9]

Recently, selective laser melting (SLM) has gained popularity as an alternative method for producing RPD frameworks and clasps. SLM fabricates components layer-by-layer by selectively melting metal powders, enabling the creation of complex geometries with high efficiency, customization, and suitability for batch production.[10-12] In recent years, various titanium alloys, including Ti-10Ta-2Nb-2Zr and Ti-6Al-4V (TC4), have attracted growing attention and have been extensively investigated for clinical applications. Among these, Ti-10Ta-2Nb-2Zr is considered a promising alternative to TC4 in orthopedic applications due to its lower elastic modulus (E) and tunable porous structure, which enable improved mechanical compatibility and effective mitigation of the stress shielding effect.[13,14] In contrast, in the field of dentistry, TC4 remains the most used alloy for fabricating RPD frameworks through SLM technology due to its high cost-effectiveness. However, because of the layer-by-layer fabrication and rapid cooling inherent in the SLM process, SLM-fabricated TC4 components typically exhibit high strength (>1,200 MPa), low ductility (<10%), and pronounced mechanical anisotropy.[15-17] These characteristics pose significant challenges for the clinical application of SLM-fabricated TC4 frameworks and have therefore limited their widespread adoption.

Heat treatment can effectively eliminate crystallographic defects such as dislocations, thereby relieving residual stress and stabilizing the microstructure.[17,18] Currently, numerous heat treatment techniques provide promising strategies for achieving a balanced combination of strength and ductility in SLM-fabricated TC4 alloy. Zou *et al.*[19] reported a rapid heat treatment process in which five cylindrical specimens were subjected to complete β-phase annealing in an argon-protected atmosphere, heated at a constant rate of 10°C/s to the target temperature of 1030°C, held for 1 s, and subsequently air-cooled to room temperature, resulting in an increase in elongation of SLM-fabricated TC4 specimens from 5.2% to 16.6%. Zhang *et al.*[20] indicated that triple heat treatments yielded tensile strength (1,019 MPa) and elongation (16.3%) values surpassing those of conventionally cast titanium alloys. Chen *et al.*[21] demonstrated that cyclic heat treatment—including an isothermal heat treatment at 950°C for 10 min followed by additional cycling between 800°C and 900°C for a total of 12 cycles—can improve ductility to over 16% while maintaining strength above 1000 MPa. With regard to heat treatment parameters, a study performed heat treatment on SLM-fabricated TC4 alloy at temperatures ranging from 650 to 1000°C for 2 h.[22] The results showed a significant decrease in strength accompanied by an increase in elongation. Furthermore, the optimal balance between strength and elongation was achieved at 900°C. Most of the aforementioned studies have employed the subcritical temperature heat treatment process (below the β-phase transformation temperature of 985.81°C for SLM-fabricated TC4 alloy[23]), effectively mitigating the strength–ductility trade-off in TC4 alloy specimens. Thus, in the dental field, optimizing the comprehensive mechanical properties of SLM-fabricated TC4 RPD frameworks through subcritical temperature heat treatment—and achieving a clinically acceptable service life—is potentially feasible.

In general, RPDs comprise clasps, artificial teeth, and bases, among which clasps are the most geometrically complex component. Clasps provide support, bracing, and retention by engaging abutment surfaces and undercuts, necessitating high fitness accuracy and sustained retentive force.[24,25] Furthermore, RPD clasps are subjected to repetitive insertion and removal, as well as continuous flexing during mastication, which may lead to permanent deformation or fatigue fracture.[26-29] Clinical survival analyses of RPDs have identified clasps as the most frequently fractured component (16.1%), markedly higher than the failure rates of minor connectors (3.4%) and major connectors (5.1%).[30] Consequently, the fitness accuracy and fatigue resistance of clasps—particularly regarding retentive force and permanent deformation—remain focal points of current studies.[27,31,32]

Researchers[33] had attempted to identify optimal heat treatment temperatures to reduce residual stress in SLM RPD cobalt–chromium (Co–Cr) frameworks in order to minimize deformation. They found that for Co–Cr alloys,

1100°C was more effective than 880°C in relieving residual stress. However, to date, no research has reported the effects of heat treatment temperature and holding time on the fitness accuracy, retention force, and permanent deformation of TC4 clasps fabricated by SLM under infrared vacuum rapid annealing conditions. Therefore, the present study focuses on SLM TC4 clasps subjected to heat treatment at various temperatures (700, 750, 800, and 850°C) and times (0.5, 1.0, and 1.5 h). Following internal quality evaluation, the effects of these parameters on clasp fitness accuracy, retentive force (before and after 10,000 simulated clinical insertion/removal cycles), and permanent deformation were assessed. The null hypothesis of this study was that varying heat treatment temperatures and times would have the same effect on the fitness accuracy, retentive force, or permanent deformation of SLM TC4 clasps.

2. Materials and methods

2.1. Sample fabrication

2.1.1. Construction of clasp-die data and die fabrication

Based on previous studies,[32,34] a molar die (specified dimensions: Diameter 10.0 mm, height 8.0 mm, and radius of curvature 7.5 mm) was designed using UG software (V8.0.0.25, Siemens Product Lifecycle Management Software Inc., Germany). The die data were then imported into Geomagic Freeform software (V2015.0.18, 3D Systems Inc., United States of America [USA]) to design the clasp model. The clasp arm featured an embracing angle of 120° and an undercut depth of 0.5 mm. A cylindrical connector was added at the clasp shoulder, and the design was saved as reference data (REF), as illustrated in Figure 1.

Subsequently, the die data were imported into a 6-axis, 5-linkage precision automatic lathe (S206A, Tsusho Precision Machinery Co., Ltd., Japan), with positioning accuracy of 1 μm on the x, y, and z axes, and repeatability within 5 μm. A stainless steel die (S46910, Sandvik AB, Sweden) was machined accordingly. The fabricated stainless steel die was used for subsequent insertion/removal cycling tests of the SLM TC4 clasps, following verification using an optical measuring instrument (JVB300C, Guiyang New Sky Optoelectronics Technology Co., Ltd., China) with a measurement resolution of 0.50 μm and measurement accuracy of (3 + L/200) μm.

2.1.2. Clasp sample fabrication

Sample size was estimated using G*Power software (V3.1.9.7, University of Düsseldorf, Germany), with an effect size of 0.35, significance level (α) of 0.05, and statistical power (1–β) of 0.8, resulting in a required sample size of 9.83/group. Accordingly, 10 specimens per group were prepared for the formal experiments.

The REF was imported into layout software (Magics V21.0, Materialis NV, Belgium), ensuring the long axis plane of the clasps was parallel to the build plate, as illustrated in Figure 2. The support density was set to 0.50 mm, the layer thickness to 0.025 mm, and a total of 141 layers were processed. A metal laser printer (MLab cusing R, Concept Laser GmbH, Germany) was used with the following settings: Wavelength 1,070 nm, spot diameter 50 μm, and laser power 100 W. The TC4 powder (YC-2.5 kg, Youcai Technology Co., Ltd., China) used for fabrication had the following composition: Ti 90%, Al 5.8–6%, V 3.8–4%, Fe 0–0.05%, H < 0.05%, with particle size 15–53 μm. Its material properties included an E of 110 GPa, 0.2% offset

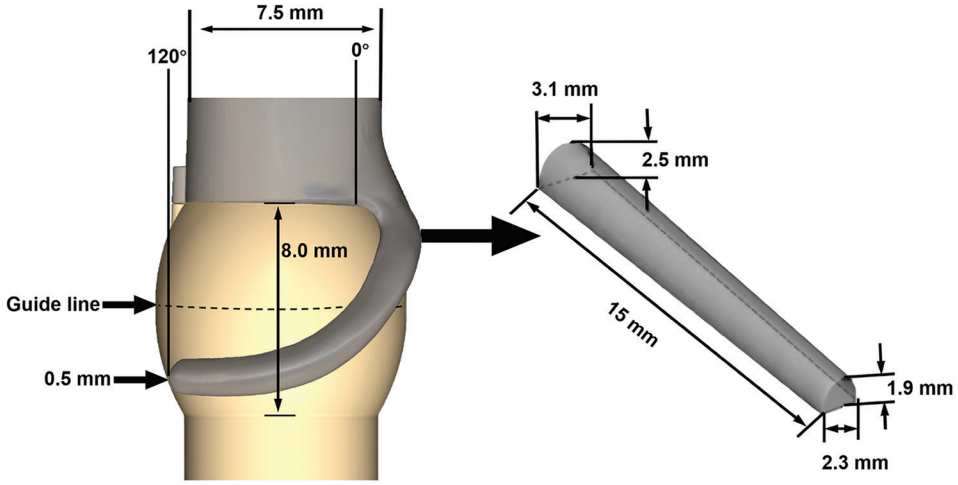

Figure 1. Design of the clasp and die.[9,32]

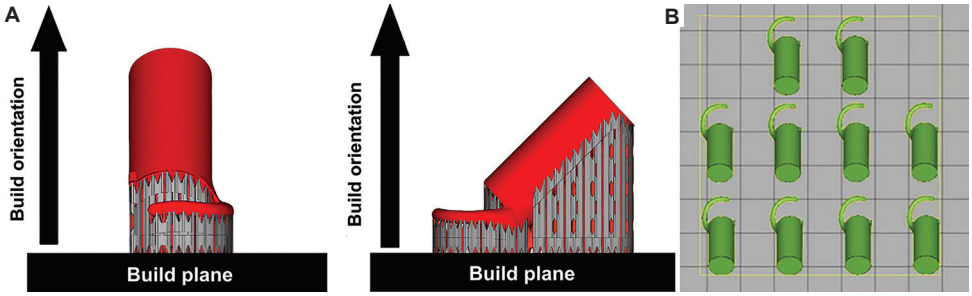

Figure 2. Build orientation and typesetting of clasps. (A) Build orientation of clasp data. (B) Typesetting of clasp data

yield strength (Rp 0.2) of 1,065 MPa, and elongation at break (A5) of 11%. In total, 120 clasp specimens (10/group) were fabricated (Figure 3). After printing, the builds were heat-treated in a vacuum annealing furnace (RZF1200-14-219, Refan High Temperature Equipment Co., Ltd., China). All heat treatment procedures were initiated from room temperature and adopted a constant heating rate to reach the target temperatures. Specifically, the temperature was ramped to 700°C over 55 min, 750°C over 60 min, 800°C over 65 min, and 850°C over 70 min. Upon reaching each target temperature, the specimens were held isothermally for 0.5 h, 1.0 h, and 1.5 h (three holding time groups per target temperature). Following the completion of the isothermal holding stage, all specimens were subjected to furnace cooling to room temperature. The heat treatment procedures are shown in Figure 4.

The clasp specimens were then removed from the building plate using an electric discharge wire-cutting machine (DK7735, Jiesheng Machinery Manufacturing Co., Ltd., China). All clasps were ground by one technician to remove support structures without subsequent polishing, only clearing obvious nodules to mitigate the impact of surface roughness.

2.2. Internal quality assessment of clasps

Internal quality of all clasp groups was evaluated using a digital X-ray imaging system (FM-C2, Anjian Technology Co., Ltd., China). The position of the X-ray lens relative to the samples was set as follows: Source-to-image distance: 100 cm; lens height: 100 cm; shooting angle: 90°; shooting range: 42 × 42 cm^2. X-ray parameters were set to an accelerating voltage of 55 kV, current of 50 mA, and exposure of 0.2 mA/s. As shown in Figure 5, all specimens exhibited uniformly dense radiographic images without obvious evidence of low-density areas such as pores or defects.

2.3. Evaluation of fitness accuracy

Clasp specimens from each group were scanned using a model scanner (E4, 3Shape A/S, Denmark) to obtain the test

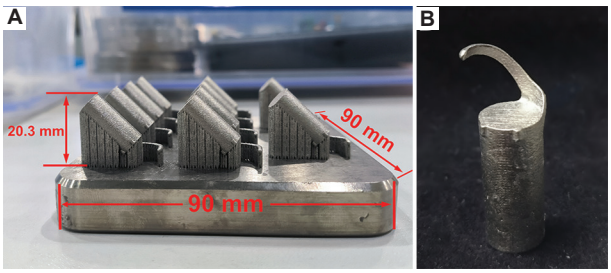

Figure 3. The selective laser melting (SLM)-fabricated TC4 clasp specimens upon completion of production. (A) The TC4 clasp specimens were fabricated by SLM on the build plate. (B) Remove the representative sample from the build plane and support structures

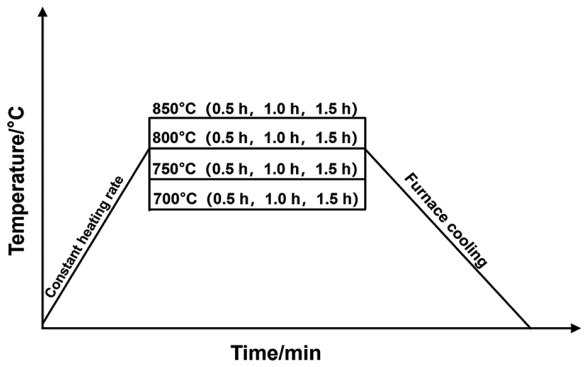

Figure 4. Schematic illustration of the heat treatment process for selective laser melting-fabricated TC4 clasps

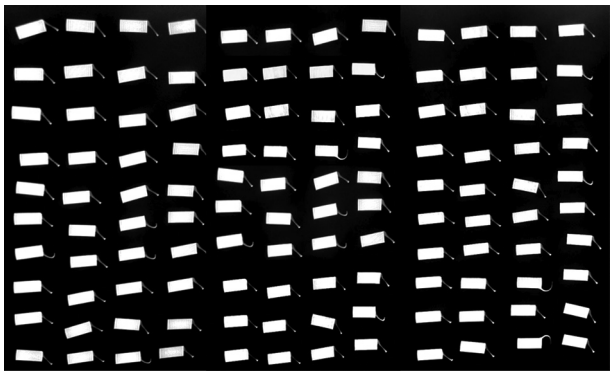

Figure 5. Digital X-ray characterization of internal quality for the selective laser melting-fabricated TC4 clasps

data. Following methods reported in previous literature,[32] both the test data and REF were imported into Geomagic Wrap software (V2017.0.1, 3D Systems, Inc., USA). First, the "Trim" function was used to segment the clasp arms and connectors from both the test data and REF, using the upper plane of the clasp as the reference. Next, the "Trim with Curve" tool was applied to draw a closed contour on the clasp arm of the REF, dividing it into two parts: inner and outer surfaces. The inner surface data were recorded as REF1. Finally, the best fit alignment of the test data with REF and the test data with REF1 was conducted, resulting in the calculation of the root mean square error (RMSE) to represent the internal and overall fitness accuracy of the clasps, respectively. In the "Deviation Analysis" function, the maximum and minimum critical thresholds were set to +500 μm and −500 μm, respectively. The RMSE was calculated according to Equation 1:[32,35]

$$\mathrm{RMSE} = \sqrt{\frac{1}{n}\sum_{i=1}^{n}\left(x_{1,i} - x_{2,i}\right)^2} \quad (1)$$

where $x_{1,i}$ represents the measurement point i on the reference model; $x_{2,i}$ represents the measurement point i on the test model; and n is the total number of measurement point pairs on each sample

2.4. Retentive force test

The clasp and die were mounted on a tensile fatigue testing machine (Model No: 8801; Instron Ltd., USA), and the fixture was adjusted to align the clasp axis with the longitudinal axis of the die. The specimens were immersed in artificial saliva (A7990, Beijing Solarbio Science & Technology Co., Ltd., China), composed of H_2O, NaCl, KCl, $CaCl_2$, NaH_2PO_4, urea, and Na_2S, at room temperature (Figure 6). In accordance with previous studies,[32,36] cyclic insertion and removal testing was conducted at a speed of 1 mm/s. The maximum dislodging force (i.e., retentive force) was recorded during clasp displacement. The mean retentive force over the initial 15 cycles was defined as the initial retentive force.[32,37,38]

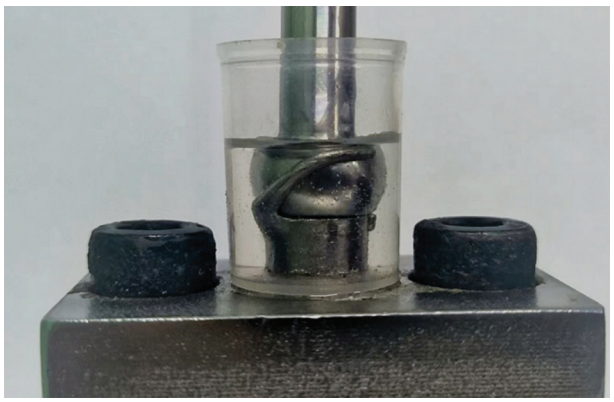

Figure 6. The test of clasp insertion and removal cycles in artificial saliva

Following the measurement of initial retentive force, each clasp was removed from the die at 16 mm/s and reinserted at the same speed, completing a total of 10,000 insertion/removal cycles. Referring to previous studies,[34,39] retentive force was recorded at the following cycle intervals: 500–514, 1000–1014, 2000–2014, 3000–3014, 4000–4014, 5000–5014, 6000–6014, 7000–7014, 8000–8014, 9000–9014, and 10,000–10,014, yielding 11 sets of data. The mean retentive force for each interval was calculated, and the final group's mean value was defined as the final retentive force. The percentage of retentive force loss was calculated according to Equation 2:

$$\text{Descent rate} = \frac{\text{Initial retentive force} - \text{Final retentive force}}{\text{Initial retentive force}} \times 100\% \quad (2)$$

To minimize bias due to localized wear of the die, each die was rotated 30° around its longitudinal axis following testing.

2.5. Permanent deformation test

Following the retentive force test, non-fractured specimens were scanned to obtain data after 10,000 insertion/removal cycles. Pre- and post-cycling test data were imported into 3D analysis software. A best-fit alignment was performed with reference to fitness accuracy analysis, and RMSE was calculated to quantify permanent deformation of the clasps.

2.6. X-ray diffraction and fracture surface analysis

For the as-built group (one sample) and each heat-treated group (one sample per group), the clasp specimens were ground using silicon carbide sandpaper up to 4000 grit and subsequently polished with diamond suspension to achieve a mirror finish. Phase analysis was performed using an X-ray diffractometer (DX-27mini, Dandong Haoyuan Instrument Co., Ltd., China) under the following conditions: scanning range of 20–80° 2θ, scanning rate of 0.02°/s, tube voltage of 40 kV, and tube current of 13 mA, with Cu Kα radiation (λ = 0.154 nm). The resulting X-ray diffraction patterns were analyzed for phase composition using Jade 6.5 software (Materials Data, Inc., USA).

Fracture surface morphology of failed specimens was examined using a scanning electron microscope (SEM; S-3000 N, Hitachi High Technologies Corp., Japan) at an accelerating voltage of 15 kV and a beam current of 50 mA.

2.7. Statistical analysis

All statistical analyses were conducted using SPSS software (version 26.0, IBM SPSS Inc., USA). The normality and homogeneity of variance for fitness accuracy, retentive force, and permanent deformation were assessed. If both assumptions were met, two-way analysis of variance (ANOVA) with Tukey's honestly significant difference *post hoc* test was applied; otherwise, the Kruskal–Wallis *H* test with Dunn's *post hoc* test with Bonferroni correction was employed. A significance level of (α) 0.05 was used for all analyses.

3. Results

3.1. Fitness accuracy

Table 1 shows the fitness accuracy of the inner surfaces and overall structures of clasps subjected to different heat treatment temperatures and times. For both the overall structure and inner surface, the 700°C/0.5 h group exhibited significantly higher RMSE values compared to other groups ($p<0.05$), indicating inferior fitness. No significant differences were observed among the remaining groups ($p>0.05$). Given that clasp fitness is an important prerequisite for its retentive and resistance to permanent deformation, to avoid errors caused by different fitness accuracies in subsequent experiments and to ensure comparability, clasps from the 700°C/0.5 h group were excluded from subsequent mechanical testing (retentive force and permanent deformation). This decision is based on the principle of controlling variables.

3.2. Retentive force

Table 2 shows the retentive force values of clasp groups subjected to different heat treatment temperatures and times. Initial retentive forces for SLM TC4 clasps ranged from 7.12 to 9.49 N, and final retentive forces after 10,000 insertion/removal cycles ranged from 6.42 to 8.83 N, reflecting a reduction rate of 4.06–12.18%.

Figure 7 shows that the retentive force of clasps subjected to different heat treatment conditions initially increased and subsequently decreased over the 10,000 cycles, with a transition phase between 500 and 2000 cycles. Furthermore, across all times (0.5, 1.0, and 1.5 h), clasps subjected to higher heat treatment temperatures exhibited progressively lower retentive forces from initial to final measurements.

Two-way ANOVA results (Table 3) revealed that heat treatment temperature had a significant effect on both initial and final retentive forces ($p<0.001$), while neither the effect of heat treatment time nor the interaction between time and temperature was statistically significant ($p>0.05$).

Figure 8 shows the interaction plots for initial and final retentive forces across heat treatment conditions. Increasing heat treatment temperature consistently resulted in decreased initial (Figure 8A) and final (Figure 8B) retentive forces across all 3 times. Notably, heat-treated clasps for 1.0 h demonstrated the lowest retentive forces across all temperature levels, compared to those treated for 0.5 h or 1.5 h. It should be noted that, given the relatively large standard deviations in both the initial and final retention forces—indicating substantial data variability—the differences among these mean values fall within an acceptable range relative to the clinically observed retention forces.

3.3. Permanent deformation

Table 4 shows the permanent deformation values of clasps after 10,000 insertion/removal cycles under different heat treatment conditions, ranging from 31.15–38.05 μm. No significant effects of heat treatment temperature or time on permanent deformation were observed ($p>0.05$).

Table 1. The root mean square error values (μm) of the inner and overall surface of fitness accuracy of clasps under different heat treatment temperatures and times

Group	700°C		750°C		800°C		850°C		*F*		*p*	
	Inner	Overall	Inner	Overall	Inner	Overall	Inner	Overall	Inner	Overall	Inner	Overall
0.5 h	75.81±11.50^{Aa}	55.52±4.68^{Aa}	60.19±9.83^{B}	46.32±5.71^{B}	67.73±14.20^{B}	45.58±7.42^{B}	65.97±10.63^{B}	45.24±6.89^{B}	3.221	7.477	0.033	0.001
1.0 h	59.57±13.05^{b}	43.70±6.39^{b}	63.29±18.84	42.92±4.52	66.55±17.72	45.30±5.46	60.45±6.31	45.59±6.37	0.402	0.509	0.753	0.678
1.5 h	65.16±16.15^{b}	46.14±7.64^{b}	69.55±11.33	47.53±5.71	65.63±7.54	46.77±6.48	67.43±16.12	49.19±6.52	0.203	0.442	0.894	0.724
F/*H*	*F*=3.931	*F*=12.541	*F*=1.058	*F*=1.99	*F*=0.052	*H*=1.058	*F*=0.860	*H*=1.271				
p	0.030	0.001	0.361	0.154	0.949	0.361	0.435	0.298				

Notes: Data are normally distributed and are presented as mean±standard deviation. Different superscript uppercase letters indicate significant differences in the whole area or inner surface fitness accuracy of clasps across different temperature groups under the same heat treatment time ($p<0.05$); ^{A}: Compared with the 750°C/0.5 h, 800°C/0.5 h, and 850°C/0.5 h groups; ^{B}: Compared with the 700°C/0.5 h group. Different superscript lowercase letters indicate significant differences in the whole area or inner surface fitness accuracy of clasps across different time groups under the same heat treatment temperature ($p<0.05$): ^{a}: Compared with the 700°C/1.0 h and 700°C/1.5 h groups; ^{b}: Compared with the 700°C/0.5 h group. n=10.

Table 2. Retentive force (N) after insertion/removal cycles under different heat treatment temperatures and times

Group	0	500	1,000	2,000	3,000	4,000	5,000	6,000	7,000	8,000	9,000	10,000	Descent rate (%)
0.5 h													
750°C	9.31±0.14	10.14±1.64	10.44±2.55	10.35±2.53	10.20±2.47	10.13±1.89	9.56±1.20	9.53±1.81	9.42±1.27	9.35±0.92	9.08±0.89	8.79±0.92	5.58
800°C	8.87±1.02	9.92±0.81	9.66±0.50	9.65±1.51	9.59±0.49	9.57±1.98	9.54±1.37	9.29±2.27	8.94±2.06	8.74±2.41	8.61±2.62	8.51±2.51	4.06
850°C	7.72±0.94	7.71±1.08	7.53±1.45	7.39±1.34	7.16±1.36	6.95±0.89	6.87±0.99	6.84±0.81	6.83±0.47	6.79±0.73	6.81±0.88	6.78±0.92	12.18
1.0 h													
700°C	9.32±0.81	9.61±0.72	9.59±0.68	9.31±0.62	8.96±0.78	8.87±0.88	8.85±0.92	8.66±0.64	8.60±0.65	8.59±0.63	8.55±0.59	8.52±0.59a	8.58
750°C	9.13±0.95	9.44±0.77	9.58±0.58	9.42±0.71	9.39±0.58	9.28±0.89	9.17±1.30	9.05±1.57	9.02±1.95	8.95±2.01	8.75±1.98	8.25±2.10	7.56
800°C	7.78±1.44	7.82±1.72	7.90±2.01	8.09±1.48	7.92±1.44	7.85±1.34	7.61±0.98	7.57±0.87	7.51±0.88	7.43±0.85	7.39±0.69	7.07±0.71	9.16
850°C	7.12±1.43	7.02±1.14	7.41±0.84	6.93±0.90	6.72±1.28	6.58±1.11	6.57±1.20	6.56±0.79	6.51±1.14	6.47±1.15	6.43±2.23	6.42±2.18	9.83
1.5 h													
700°C	9.49±1.63	10.78±1.83	10.28±2.67	9.87±2.83	9.75±2.62	9.53±2.59	9.44±2.27	9.33±2.15	9.02±1.52	8.96±1.71	8.93±1.34b	8.83±1.21	7.00
750°C	9.45±2.16	10.32±1.89	9.91±1.29	9.91±0.93	9.89±0.86	9.71±0.84	9.63±0.82	9.58±0.81	9.33±0.96	9.15±0.81	8.88±0.65	8.77±0.27	7.75
800°C	8.74±2.73	9.28±2.02	9.88±2.55	9.85±2.17	9.73±2.24	9.66±2.37	9.47±2.39	9.37±2.36	9.03±2.36	8.88±2.27	8.66±2.07	8.22±1.83	5.94
850°C	7.78±2.39	9.21±2.53	9.38±2.61	9.13±2.24	8.63±1.82	8.49±1.41	7.84±2.52	7.81±2.47	7.49±2.87c	7.18±2.61	7.08±1.73	7.06±1.93	9.25

Note: Data are normally distributed and are expressed as mean±standard deviation. a indicates that the data from the 700 °C/1.0 h group beyond this cycle (inclusive) exclude sample 10; b indicates that the data from the 700 °C/1.5 h group beyond this cycle (inclusive) exclude sample 2; c indicates that the data from the 850 °C/1.5 h group beyond this cycle (inclusive) exclude sample 1. These data were excluded because the samples fractured after the corresponding cycles. n=10.

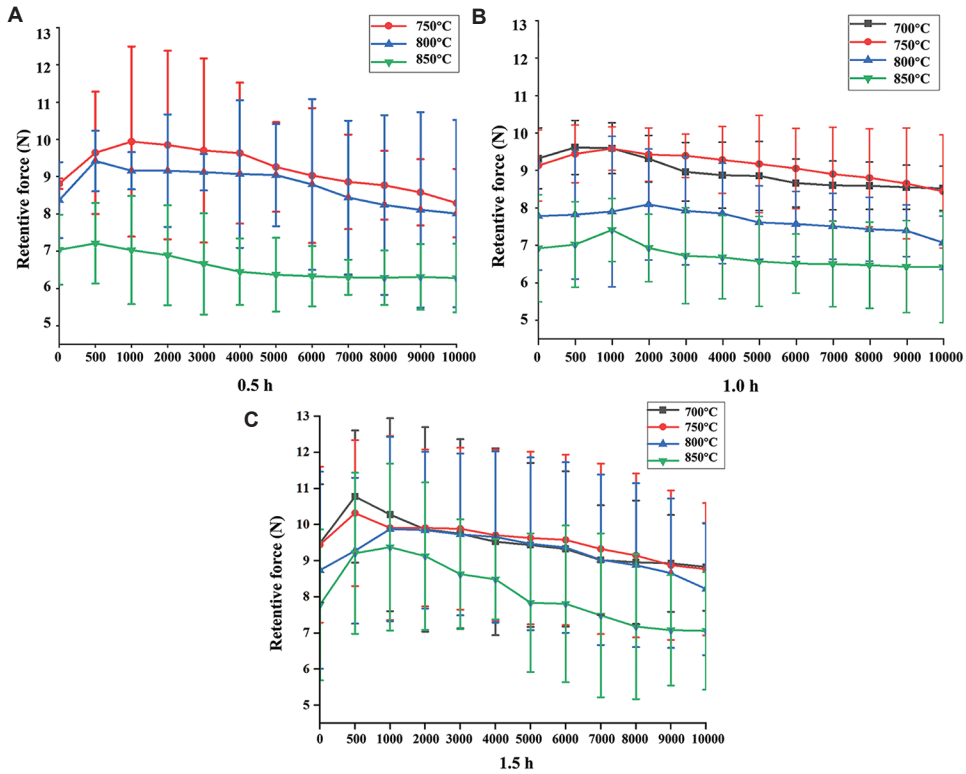

Figure 7. Retentive force of each clasp group after 10,000 insertion/removal cycles under different heat treatment temperatures and times. (A) 0.5 h group. (B) 1.0 h group. (C) 1.5 h group

Table 3. Two-way analysis of variance of the effects of heat treatment temperature and time on the initial or final retentive force of the clasp

Independent variable	Sum of squares	Degree of freedom	Mean square root	*F*	*p*
Initial retentive force					
Time	8.626	2	3.683	1.297	0.278
Temperature	91.112	3	21.185	7.462	<0.001
Temperature * time	4.052	5	0.609	0.215	0.956
Final retentive force					
Time	14.137	2	7.282	2.791	0.066
Temperature	78.504	3	22.108	8.475	<0.001
Temperature * time	16.367	5	1.465	0.562	0.729

Note: Degree of freedom (n-1). F variation between sample means / variation within samples. The asterisk (*) denotes the interaction effect between heat treatment temperature and time in the two-way analysis of variance.

As shown in the interaction plot (Figure 9), the mean differences in permanent deformation across groups are minimal, suggesting that neither heat treatment temperature nor time had a significant effect on permanent deformation in this study. It should be noted that the relatively large standard deviations of permanent deformation values—markedly deviating from the mean—in groups with lower heat treatment temperatures or shorter time (700°C/1.5 h and 800°C/0.5 h) indicate substantial variability and poor stability of the data. Therefore, these findings should be interpreted with caution and integrated carefully with clinical practice.

The color-coded image illustrating the permanent deformation of the clasps is shown in Figure 10. As can be observed from the figure, the permanent deformation of the clasp gradually increased from the middle section to the end (i.e., the portion entering the die undercut), predominantly appearing in yellow, with the degree of color deviation increasing from approximately 10 μm at the center to 100 μm at the tip. In contrast, no permanent deformation was observed in the remaining regions of the specimen outside the clasp, which appeared green.

3.4. X-ray diffraction and scanning electron microscope observation of the fracture surface

Figure 11 presents the X-ray diffraction patterns of untreated (as-built) and heat-treated TC4 clasp specimens. Compared with the as-built sample, the heat-treated samples exhibited higher diffraction peak intensities and a narrower full width at half maximum for the α-Ti phase. Moreover, with increasing heat treatment temperature

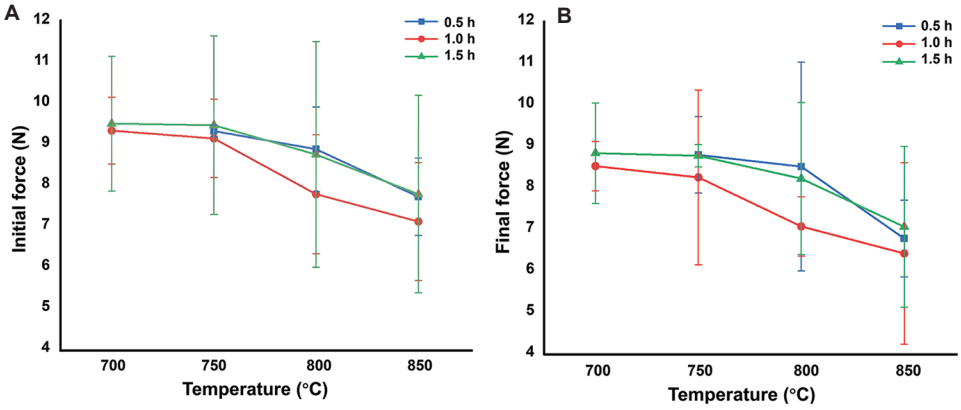

Figure 8. Interaction analysis diagram of the retentive force of the clasp with respect to the heat treatment temperature and time. (A) The initial and (B) final retentive forces of clasps

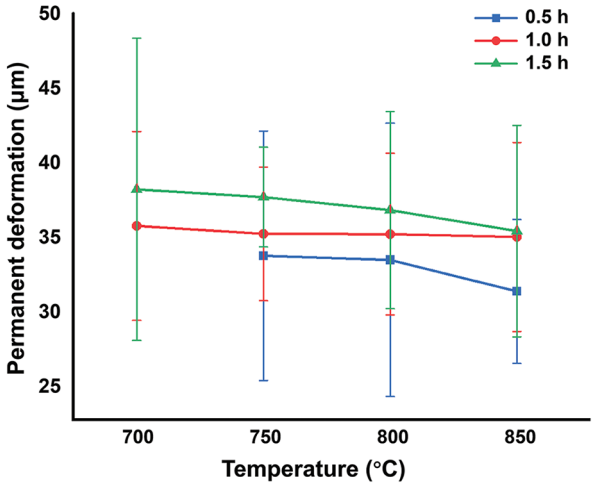

Figure 9. Interaction analysis diagram of permanent deformation

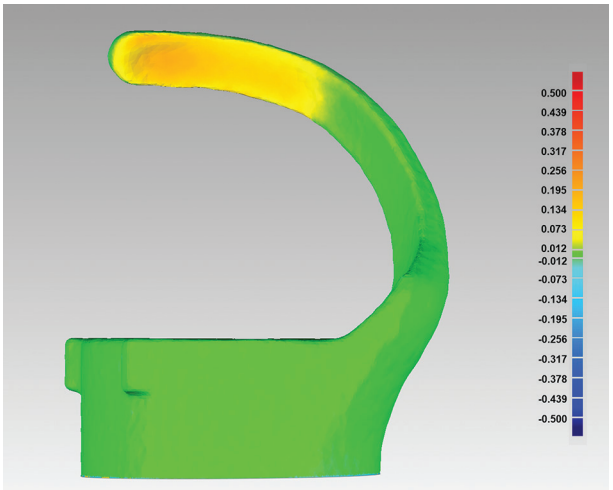

Figure 10. Color-coded image of permanent deformation for the representative TC4 clasp sample

Table 4. Root mean square error values (μm) of permanent deformation of clasps at different heat treatment temperatures and times

Group	700°C	750°C	800°C	850°C	*F*	*p*
0.5 h	-	33.56±8.43	33.28±9.24	31.15±4.87	0.260	0.773
1.0 h	35.58±6.39	35.04±4.52	35.02±5.46	34.83±6.39	0.029	0.993
1.5 h	38.05±10.22	37.53±3.37	36.65±6.67	35.23±7.15	0.224	0.879
F	0.378	1.057	0.489	1.196		
p	0.546	0.362	0.618	0.317		

Notes: Data are normally distributed and are expressed as mean±standard deviations."-" indicates the exclusion of the 700°C/0.5 h group from the analysis

or prolonged holding time, the diffraction peaks of the α-Ti phase progressively intensified, accompanied by a reduction in peak width and a shift in diffraction angles. These observations indicate that elevated processing temperatures and extended holding times promote the ordered growth and structural densification of α-Ti grains. However, regardless of heat treatment, all clasp samples predominantly displayed the same characteristic diffraction peaks of the α-Ti phase within the 20–80° 2θ range, indicating that no significant phase transformation occurred in the TC4 clasps under the annealing conditions of 700–850°C and holding durations of 0.5–1.5 h.

Figure 12 shows the macroscopic morphology of a failed specimen, revealing a fracture at the middle portion of the clasp arm. SEM examination of a representative failed specimen from the 700°C/1.0 h group (Figure 13) revealed several structural defects: Porosities, incompletely melted metal powders, and cracks on the fracture plane (Figure 13A); a distinct crack in the left region at higher magnification (Figure 13B); coexisting porosities and

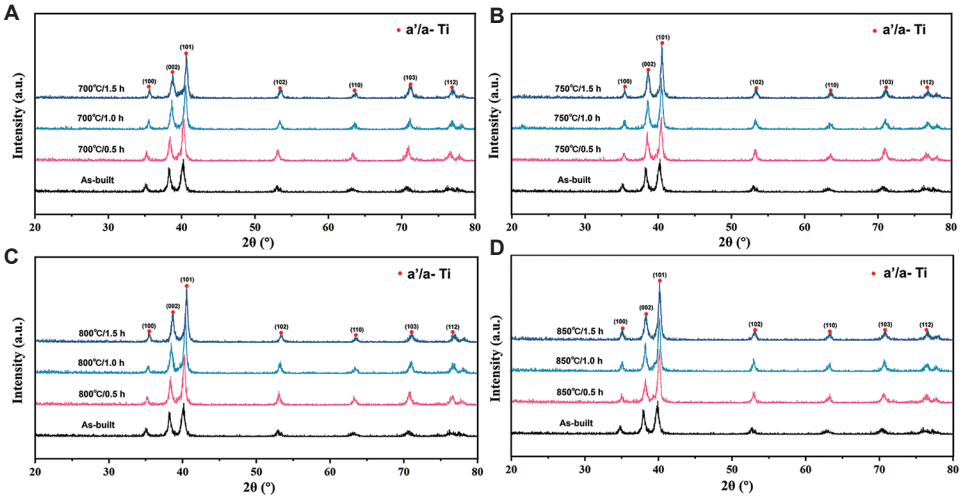

Figure 11. X-ray diffraction patterns of as-built and heat-treated TC4 samples. (A) 700°C/0.5, 1.0, 1.5 h. (B) 750°C/0.5, 1.0, 1.5 h. (C) 800°C/0.5, 1.0, 1.5 h. (D) 850°C/0.5, 1.0, 1.5 h

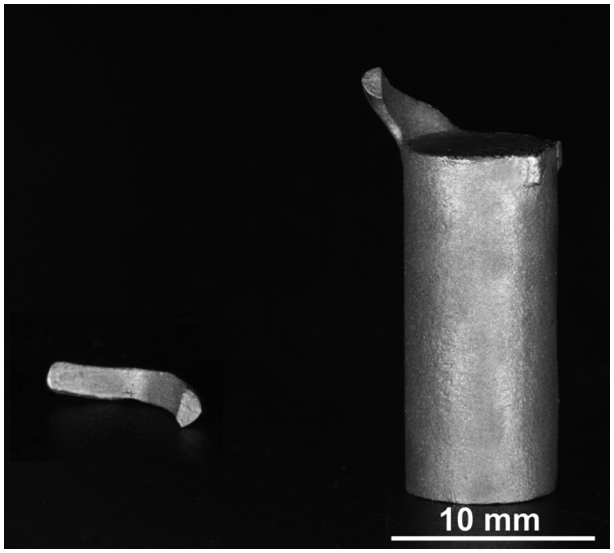

Figure 12. Broken clasp sample

cracks in the upper section (Figure 13C); incompletely melted metal powders in the upper-right zone (Figure 13D); crack, incompletely melted metal powders and porosity in the lower-right region (Figure 13E); and incompletely melted metal powders in the bottom edge (Figure 13F).

4. Discussion

The conventional annealing furnace treatment process poses a risk of hydrogen embrittlement in titanium alloys due to the presence of impurities, which facilitate the uptake of hydrogen (H), oxygen (O), nitrogen (N), and other elements.[40] In contrast, vacuum heat treatment effectively prevents the ingress of reactive elements such as hydrogen, thereby significantly inhibiting embrittlement.[41] This study employed an infrared-heated vacuum system for precise temperature control, improved efficiency, and effective elimination of atmospheric hydrogen. Based on previous reports,[42] annealing heat treatment of TC4 alloys fabricated by SLM was typically performed at 600–750°C for 2 h. In contrast, for other non-annealing heat treatments under the same holding duration (2 h), the appropriate temperature range was 800–900°C. Considering the operational constraints of the vacuum infrared heat treatment equipment used in this study, heat treatment effects within a temperature range of 700–850°C and holding times of 0.5–1.5 h were systematically investigated. Results showed that temperature and time significantly influenced clasp fitness accuracy and retentive force, while permanent deformation remained largely unchanged. Thus, the null hypothesis is partially rejected.

All clasps in this study were printed using uniform parameters and randomly numbered to minimize the influence of surface roughness on retentive force. The heat treatment temperature was kept well below the melting point of TC4 (around 1660°C[43]), preventing any surface alteration due to melting. Given our group's previous focus on clasp surface roughness (Ra 8.28–9.90 μm[32]) and the above considerations, this study did not include surface roughness measurements. Conventional clasps often have reciprocal arms and retentive arms. However, in this study, the clasp design was simplified by including only the retentive arm, omitting the reciprocal arm to prevent any interference during insertion/removal and retentive force testing. In addition, the clasp's undercut depth was set at 0.5 mm, a value supported by previous research,[25,44] indicating that this depth provides suitable retentive force for titanium alloy clasps.

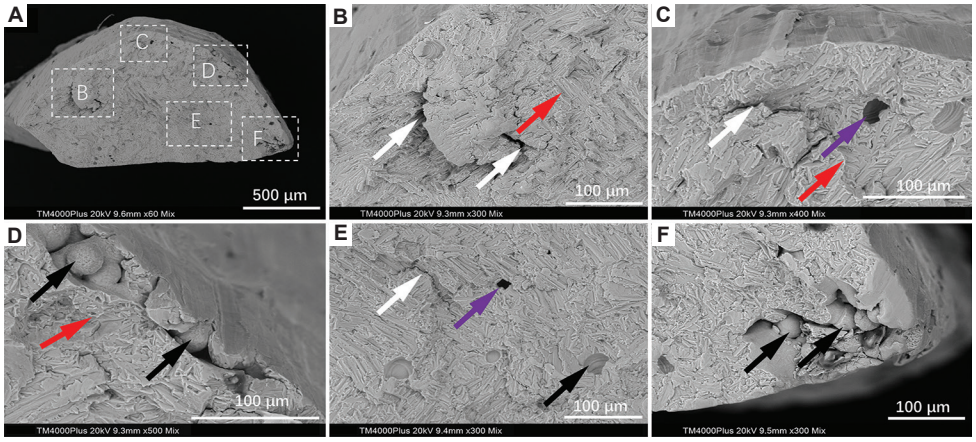

Figure 13. The scanning electron microscopy observation of the fracture surface of a failed clasp. (A) Fracture surfaces of clasp arm (scale bar: 500 μm; magnification: ×60). (B) Left side (scale bar: 100 μm; magnification ×300), (C) upper side (scale bar: 100 μm; magnification ×400), (D) upper-right side (scale bar: 100 μm; magnification ×500), (E) lower-right side (scale bar: 100 μm; magnification ×300), and (F) internal and external surface corners of the fracture surface of the clasp (scale bar: 100 μm; magnification ×300)
Notes: White arrows represent cracks; Black arrows represent incompletely melted powder; Purple arrows represent pores or defects; Red arrows represent cleavage fracture

The fitness accuracy of clasps is crucial for the passive seating of RPDs and improved clinical outcomes.[45] However, SLM fabrication often induces residual stresses from melt-cooling shrinkage, leading to deformation.[46,47] Under the rapid solidification and cooling rates (can reach 10^8 K/s) of SLM, body-centered cubic β-phase of TC4 alloy transforms completely into metastable hexagonal close-packed α′-phase by a diffusionless, shear-type transformation process,[48] introducing additional phase transformation stresses and further complicating the residual stress.[9,49] To mitigate this, beyond optimizing support structures, specific heat treatments have been shown to effectively relieve these stresses in TC4 specimens and reduce deformation.[50,51] Previous studies confirmed that prolonged heat treatment durations are particularly effective in minimizing residual stress in SLM-processed pure titanium and its alloys.[52,53] Furthermore, residual stresses in TC4 titanium decrease progressively with increasing heat treatment temperature and can be nearly eliminated when exceeding 750°C.[54-56]

In this study, different heat treatment parameters significantly affected the fitness accuracy of the SLM-fabricated clasps. Specifically, the group treated with 700°C for 0.5 h showed the poorest accuracy (55.52 ± 4.68 μm), with a statistically significant difference from other groups. This is likely because the temperature and duration at 700°C were insufficient to fully relieve internal residual stresses,[56] thus compromising the final precision of the clasps. The reported fitness accuracy of SLM-fabricated TC4 clasps varies across studies. Previous studies have reported values of 50.95 ± 5.79 μm,[32] which are consistent with those observed in the present study (mean: 42.92–55.52 μm). However, other studies have reported higher values, reaching 86 ± 9 μm[57] and 97.45 ± 32.58 μm.[58] These discrepancies are likely due to differences in processing parameters, location of the research subject, and measurement techniques employed in the respective studies. Currently, no unified clinical threshold exists for micrometer-level fitness accuracy. However, since fitness accuracy critically influences properties such as retentive force and permanent deformation, the 700°C/0.5 h group was excluded from these tests to minimize the impact of its poor fitness accuracy on subsequent results.

Clasp retentive force is influenced by multiple factors, including undercut depth, arm length, thickness, and material properties.[57] Previous studies have performed annealing treatments on SLM-fabricated TC4 alloy at 650–1000°C[23] and 750–1050°C[22] for 2 h, revealing that the compressive strength, tensile strength, and microhardness of the alloy significantly decreased, while elongation increased. This indicates that increasing the heat treatment temperature reduces the strength and hardness of the TC4 alloy, enhances its plasticity, and thereby weakens its resistance to deformation. Consequently, the reduction in frictional force during clasp disengagement from the undercut area may significantly contribute to the decrease in retentive force.[31] In our study, although the data exhibited a relatively large standard deviation, two-way ANOVA revealed that heat treatment temperature had a significant effect on the mean values of both initial and final retentive force. Notably, variations in heat treatment duration (0.5–1.5 h) did not significantly affect retentive force, indicating its minor role in clasp performance. This finding suggests that, clinically, heat treatment time

can be shortened without compromising quality, thereby improving the production efficiency of RPD frameworks via SLM. When the heat treatment time is set at 0.5 h, the retentive force of TC4 clasps treated within the temperature range of 750–850°C meets clinical requirements.

The typical replacement cycle for RPDs is approximately 5 years.[58,59] Based on four insertion/removal cycles per day, this corresponds to about 7250 cycles.[44] To enhance testing reliability, this study employed 10,000 cycles, consistent with previous studies.[32,60] The initial retentive forces across different heat treatment groups ranged from 7.12–9.49 N, declining to 6.42–8.83 N after testing, representing a reduction of 4.06–12.18%. It is generally believed that a total retentive force of 20 N for an RPD, typically equipped with 2–4 clasps, is sufficient during mastication of adhesive foods and is conducive to the patient's smooth removal and insertion of the RPD.[61] While ideal clasp retention may vary depending on study conditions such as clasp design and experimental environment, the commonly recommended retentive force for a single clasp is 5–10 N.[24,32,60-63] In this study, both the initial (7.12–9.49 N) and final (6.42–8.83 N) retentive forces under various heat treatment conditions fell within clinically acceptable ranges, confirming the clinical suitability of heat-treated SLM TC4 clasps.

Permanent deformation is another key clinical parameter in evaluating the effectiveness of RPDs. During the repeated insertion and removal of RPD clasps, their deformation behavior is primarily governed by yield strength and hardness. A previous study has shown that post-treatment at 780°C maintains high yield strength (1,038 MPa).[64] In contrast, treatment at 920°C promotes grain growth, leading to reduced yield strength (976 MPa). Clearly, increasing the heat treatment temperature decreases the yield strength of TC4 alloy, thereby impairing strain recovery upon unloading. Consequently, even when the applied disengagement force does not exceed the ultimate strength of the TC4 clasp, plastic deformation may still occur, manifesting as partial or complete inability to recover strain upon unloading—i.e., permanent deformation.[65] In addition, research has demonstrated that heat treatment within the elevated temperature range of 750–1050°C for a duration of 2 h facilitates a more complete annealing of the α'-martensite phase, thereby leading to a significant reduction in the microhardness of the TC4 alloy.[22] Clasps with lower hardness are more susceptible to wear, further increasing the risk of permanent deformation.[66] These findings suggest a multifactorial mechanism by which heat treatment influences permanent deformation. Although data regarding the effects of heat treatment temperature or time remain limited, the present study demonstrated minimal differences in permanent deformation (31.15–38.05 μm) among groups after 10,000 insertion/removal cycles. Compared with previous studies (29.86–52.34 μm) conducted under different conditions,[29,67] the results of our study were consistent. Thus, the effects of heat treatment temperature and time on permanent deformation appear to be limited, with all observed values remaining within clinically acceptable thresholds.

The deformation behavior of the clasp follows the principles of elastoplastic mechanics. It is governed by the relationship between the actual displacement and the material's critical elastic limit displacement threshold. In this study, the engagement depth of the TC4 clasp into the undercut was set at 0.50 mm (in the horizontal direction). If the clasp fully recovers its original shape upon unloading, this indicates the absence of permanent deformation during cyclic loading, and the actual horizontal displacement remains at 0.50 mm. Conversely, if the clasp fails to fully recover or only partially returns to its initial configuration after unloading, it signifies that plastic deformation has occurred during loading (deformation ≤0.50 mm), resulting in a reduction of the actual horizontal displacement to <0.50 mm. Notably, although an increase in permanent deformation leads to a decrease in actual displacement, it substantially enhances the fatigue life of the clasp.[32,68,69] Based on this, the limited number of clasp fractures observed in this study may be attributed to large effective displacements, with fatigue failure occurring when these displacements exceed the component's endurance limit.

Several studies have proposed that clasp fractures are commonly associated with internal and external defects as well as excessive loading forces.[43,70,71] In this study, SEM revealed surface-near defects—such as unmelted powder particles and pores—on fractured clasps from the 700°C/1.0 h, 700°C/1.5 h, and 850°C/1.5 h groups. Fracture cracks and steps were found adjacent to these defects. Moreover, a study has shown that the larger and more superficial these defects are, the more likely they are to serve as stress concentrators, promoting crack initiation and fatigue failure.[72] The frequent presence of such surface-near defects in the fractured specimens of this study may constitute the principal cause of fatigue fracture.

The present study has several limitations. First, the findings are applicable only to SLM TC4 clasps, as optimal heat treatment temperatures and times vary across different metal materials. Future studies should evaluate the effects of heat treatment temperature and time on other metal types—employing techniques such as electron backscatter diffraction to analyze crystallographic orientation and microstructure—to further expand the body of knowledge concerning the impact of heat treatment on SLM RPD

clasps and to provide more robust theoretical guidance for clinical application. Moreover, this study focused solely on clasp fitness accuracy, retentive force, and permanent deformation, without evaluating the influence of heat treatment on the overall RPD framework. Finally, as an *in vitro* investigation, although efforts were made to simulate the oral environment, this study could not fully replicate intraoral conditions. Future studies should include *in vivo* evaluations of clasp performance and the development of more accurate oral simulation protocols to establish a more reliable evidence base for clinical practice.

5. Conclusion

Under the conditions of this study, the following conclusions can be drawn:

(i) Different heat treatment temperatures and times exert varying effects on the fitness accuracy of SLM TC4 clasps. Specifically, the 700°C/0.5 h group exhibited the poorest results ($p<0.05$), whereas the remaining groups demonstrated consistent fitness accuracy.

(ii) Heat treatment temperature significantly affected both the initial and final retentive forces ($p<0.001$). In contrast, variations in heat treatment time showed no substantial influence. Notably, the initial and final retentive forces of all clasps across different heat treatment conditions met clinical requirements over 10,000 insertion/removal cycles.

(iii) Different heat treatment temperatures and times had no significant effect on permanent deformation ($p>0.05$). After 10,000 insertion/removal cycles, all groups exhibited permanent deformation within clinically acceptable limits.

(iv) After heat treatment at 750–850°C for 0.5 h, the SLM TC4 clasps meet clinical requirements in terms of fitness accuracy, retentive force, and permanent deformation, while also demonstrating high heat treatment efficiency.

(v) Internal defects generated during the printing process (including cracks and incomplete powder fusion) may be the primary cause of fracture failure in a very small number of SLM-fabricated TC4 clasps after heat treatment.

Acknowledgments

The authors specially thank the Chongqing Jingmei Medical Technology Co., Ltd., for providing the sample processing platform and the related equipment and technical support.

Funding

This study was supported by the Technology Innovation and Application Development Program of Chongqing Science and Technology Bureau (cstc2020jscx-sbqwX0006) and the 2023 medical education research project of the medical education branch of the Chinese Medical Association and the National Center for the development of medical education (No.2023A50).

Conflict of interest

Peng Wang and Lu Liu are employees of Chongqing Jingmei Medical Technology Co., Ltd.; however, they were not involved in any activities that could constitute a conflict of interest in relation to this study. We declare that we have no personal relationships with other people or organizations that can inappropriately influence our work. There are also no potential conflicts of interest in terms of employment, consultancies, ownership, honoraria, paid expert testimony, patent applications/registrations, and grants or other funding.

Author contributions

Conceptualization: Fa-Bing Tan, Na Yu
Formal analysis: Lu-Xiang Yu, Jing-Jing Fan
Investigation: Lu-Xiang Yu, Jing-Jing Fan
Methodology: Lu-Xiang Yu, Peng Wang, Lu Liu
Writing – original draft: Lu-Xiang Yu, Na Yu
Writing – review & editing: Fa-Bing Tan, Na Yu

Ethics approval and consent to participate

Not applicable.

Consent for publication

Not applicable.

Availability of data

The data that support the findings of this study are available from the corresponding author on reasonable request.

References

1. Ohkubo C, Hanatani S, Hosoi T. Present status of titanium removable dentures - a review of the literature. *J Oral Rehabil*. 2008;35(9):706-714.

   doi: 10.1111/j.1365-2842.2007.01821.x

2. Ohkubo C, Sato Y, Nishiyama Y, Suzuki Y. Titanium removable denture based on a one-metal rehabilitation concept. *Dent Mater J*. 2017;36(5):517-523.

   doi: 10.4012/dmj.2017-137

3. Da Silva L, Martinez A, Rilo B, Santana U. Titanium for removable denture bases. *J Oral Rehabil*. 2000;27(2):131-135.

   doi: 10.1046/j.1365-2842.2000.00506.x

4. Miyazaki T, Hotta Y, Kunii J, Kuriyama S, Tamaki Y. A review

of dental CAD/CAM: current status and future perspectives from 20 years of experience. *Dent Mater J*. 2009;28(1):44-56.

doi: 10.4012/dmj.28.44

5. Qiu J, Liu W, Wu D, Qiao F, Sui L. Fit accuracy in the rest region of RPDs fabricated by digital technologies and conventional lost-wax casting: A systematic review and meta-analysis. *BMC Oral Health*. 2023 23(1):667.

doi: 10.1186/s12903-023-03348-6

6. Watanabe I, Watanabe E, Yoshida K, Okabe T. Effect of surface contamination on adhesive bonding of cast pure titanium and Ti-6Al-4V alloy. *J Prosthet Dent*. 1999;81(3):270-276.

doi: 10.1016/s0022-3913(99)70268-4

7. Baltag L, Watanabe K, Kusakari H, Miyakawa O. Internal porosity of cast titanium removable partial dentures: Influence of sprue direction on porosity in circumferential clasps of a clinical framework design. *J Prosthet Dent*. 2002;88(2):151-158.

doi: 10.1067/mpr.2002.127400

8. Rodrigues RCS, Faria ACL, Orsi IA, De Mattos MDC, Macedo AP, Ribeiro RF. Comparative study of two commercially pure titanium casting methods. *J Appl Oral Sci*. 2010;18(5):487-492.

doi: 10.1590/s1678-77572010000500010

9. Takahashi K, Torii M, Nakata T, Kawamura N, Shimpo H, Ohkubo C. Fitness accuracy and retentive forces of additive manufactured titanium clasp. *J Prosthodont Res*. 2020;64(4):468-477.

doi: 10.1016/j.jpor.2020.01.001

10. Gao BW, Zhao HJ, Peng LQ, Sun ZX. A review of research progress in selective laser melting (SLM). *Micromachines (Basel)*. 2023;14(1):57.

doi: 10.3390/mi14010057

11. Kessler A, Hickel R, Reymus M. 3D printing in dentistry-state of the art. *Oper Dent*. 2020;45(1):30-40.

doi: 10.2341/18-229-l

12. Lindner M, Hoeges S, Meiners W, *et al*. Manufacturing of individual biodegradable bone substitute implants using selective laser melting technique. *J Biomed Mater Res Part A*. 2011;97A(4):466-471.

doi: 10.1002/jbm.a.33058

13. Polozov I, Nefyodova V, Zolotarev A, Popovich A. Microstructural evolution and mechanical properties of laser-powder bed fusion-fabricated Ti-10Ta-2Nb-2Zr alloy as a potential orthopedic implant material. *Mater Sci Addit Manuf*. 2025;4(3):025220044.

doi: 10.36922/msam025220044

14. Zhenhuan W, Yu D, Junsi L, *et al*. Physiochemical and biological evaluation of SLM-manufactured Ti-10Ta-2Nb-2Zr alloy for biomedical implant applications. *Biomed Mater*. 2020;15(4):045017.

doi: 10.1088/1748-605X/ab7ff4

15. Sabban R, Bahl S, Chatterjee K, Suwas S. Globularization using heat treatment in additively manufactured Ti-6Al-4V for high strength and toughness. *Acta Mater*. 2019;162:239-254.

doi: 10.1016/j.actamat.2018.09.064

16. Liu JW, Zhang K, Gao X, *et al*. Effects of the morphology of grain boundary α-phase on the anisotropic deformation behaviors of additive manufactured Ti-6Al-4V. *Mater Des*. 2022;223:111150.

doi: 10.1016/j.matdes.2022.111150

17. Wang CS, Lei Y, Li CL. Achieving an excellent strength and ductility balance in additive manufactured Ti-6Al-4V alloy through multi-step high-to-low-temperature heat treatment. *Materials (Basel)*. 2023;16(21):6947.

doi: 10.3390/ma16216947

18. Gushchina M, Turichin G, Klimova-Korsmik O, Babkin K, Maggeramova L. Features of heat treatment the Ti-6Al-4V GTD blades manufactured by DLD additive technology. *Materials (Basel)*. 2021;14(15):4159.

doi: 10.3390/ma14154159

19. Zou ZY, Simonelli M, Katrib J, Dimitrakis G, Hague R. Refinement of the grain structure of additive manufactured titanium alloys via epitaxial recrystallization enabled by rapid heat treatment. *Scr Mater*. 2020;180:66-70.

doi: 10.1016/j.scriptamat.2020.01.027

20. Zhang S, Zhang YQ, Zou ZY, Shi YS, Zang Y. The microstructure and tensile properties of additively manufactured Ti-6Al-2Zr-1Mo-1V with a trimodal microstructure obtained by multiple annealing heat treatment. *Mater Sci Eng A Struct Mater Prop Microstruct Process*. 2022;831:142241.

doi: 10.1016/j.msea.2021.142241

21. Chen J, Fabijanic D, Brandt M, Zhao Y, Ren SB, Xu W. Dynamic α globularization in laser powder bed fusion additively manufactured Ti-6Al-4V. *Acta Mater*. 2023;255:119076.

doi: 10.1016/j.actamat.2023.119076

22. Wang D, Wang H, Chen XJ, *et al*. Densification, tailored microstructure, and mechanical properties of selective laser melted Ti-6Al-4V alloy via annealing heat treatment. *Micromachines (Basel)*. 2022;13(2):331.

doi: 10.3390/mi13020331

23. Ahn B. Microstructural tailoring and enhancement in compressive properties of additive manufactured Ti-6Al-4V alloy through heat treatment. *Materials (Basel)*. 2021;14(19):5524.

doi: 10.3390/ma14195524

24. Fathy SM, Emera RMK, Abdallah RM. Surface microhardness, flexural strength, and clasp retention and deformation of acetal vs poly-ether-ether ketone after combined thermal cycling and pH aging. *J Contemp Dent Pract*. 2021;22(2):140-145.

doi: 10.5005/jp-journals-10024-2937

25. Zhang MM, Gan N, Qian HX, Jiao T. Retentive force and fitness accuracy of cobalt-chrome alloy clasps for removable partial denture fabricated with SLM technique. *J Prosthodont Res*. 2022;66(3):459-465.

doi: 10.2186/jpr.jpr_d_21_00017

26. Mahmoud AAA, Wakabayashi N, Takahashi H. Prediction of permanent deformation in cast clasps for denture prostheses using a validated nonlinear finite element model. *Dent Mater*. 2007;23(3):317-324.

doi: 10.1016/j.dental.2005.10.012

27. Benso B, Kovalik AC, Jorge JH, Campanha NH. Failures in the rehabilitation treatment with removable partial dentures. *Acta Odontol Scand*. 2013;71(6):1351-1355.

doi: 10.3109/00016357.2013.777780

28. Brandt S, Winter A, Lauer HC, Romanos G. Retrospective clinical study of 842 clasp-retained removable partial dentures with a metal framework: Survival, maintenance needs, and biologic findings. *Quintessence Int*. 2024;55(9):704-711.

doi: 10.3290/j.qi.b5566187

29. El-Tamimi KM, Bayoumi DA, Alshenaiber R, Aljulayfi I, Ahmed MMZ, El-Sayed ME. Deformation and retentive forces variations of the additively manufactured cobalt-chromium and titanium alloys dental clasps. *Saudi Dent J*. 2024;36(6):947-953.

doi: 10.1016/j.sdentj.2024.04.001

30. Behr M, Zeman F, Passauer T, *et al*. Clinical performance of cast clasp-retained removable partial dentures: A retrospective study. *Int J Prosthodont*. 2012;25(2):138-144.

doi: 10.1016/j.joen.2011.12.003

31. Zheng J, Aarts JM, Ma SY, Waddell JN, Choi JJE. Different Undercut depths influence on fatigue behavior and retentive force of removable partial denture clasp materials: A systematic review. *J Prosthodont*. 2023;32(2):108-115.

doi: 10.1111/jopr.13519

32. Tan FB, Song JL, Wang C, Fan YB, Dai HW. Titanium clasp fabricated by selective laser melting, CNC milling, and conventional casting: A comparative *in vitro* study. *J Prosthodont Res*. 2019;63(1):58-65.

doi: 10.1016/j.jpor.2018.08.002

33. Yan X, Lin H, Wu Y, Bai W. Effect of two heat treatments on mechanical properties of selective-laser-melted Co-Cr metal-ceramic alloys for application in thin removable partial dentures. *J Prosthet Dent*. 2018;119(6): 1028.e1-1028.e6.

doi: 10.1016/j.prosdent.2018.04.002

34. Xie WQ, Zheng MH, Wang JQ, Li XY. The effect of build orientation on the microstructure and properties of selective laser melting Ti-6Al-4V for removable partial denture clasps. *J Prosthet Dent*. 2020;123(1):163-172.

doi: 10.1016/j.prosdent.2018.12.007

35. Hussein MO, Hussein LA. Trueness of 3D printed partial denture frameworks: Build orientations and support structure density parameters. *J Adv Prosthodont*. 2022;14(3):150-161.

doi: 10.4047/jap.2022.14.3.150

36. Nakata T, Shimpo H, Ohkubo C. Clasp fabrication using one-process molding by repeated laser sintering and high-speed milling. *J Prosthodont Res*. 2017;61(3):276-282.

doi: 10.1016/j.jpor.2016.10.002

37. Shimpo H. Effect of arm design and chemical polishing on retentive force of cast titanium alloy clasps. *J Prosthodont*. 2010;17(4):300-307.

doi: 10.1111/j.1532-849X.2007.00289.x

38. Tokue A, Hayakawa T, Ohkubo C. Fatigue resistance and retentive force of cast clasps treated by shot peening. *J Prosthodont Res*. 2013;57(3):186-194.

doi: 10.1016/j.jpor.2013.01.006

39. Zhu YH, Zhang B, Liu YH, Qin F, Li HF, Zheng YF. [Fracture analyses of casting framework removable partial dentures]. *Beijing Da Xue Xue Bao Yi Xue Ban*. 2012;44(1):80-83.

doi: 10.3969/j.issn.1671-167x.2012.01.017

40. Ghouse S, Oosterbeek RN, Mehmood AT, Vecchiato F, Dye D, Jeffers JRT. Vacuum heat treatments of titanium porous structures. *Addit Manuf*. 2021;47:102262.

doi: 10.1016/j.addma.2021.102262

41. Wang QP, Kong J, Liu XK, *et al*. The effect of a novel low-temperature vacuum heat treatment on the microstructure and properties of Ti-6Al-4V alloys manufactured by selective laser melting. *Vacuum*. 2021;193:110554.

doi: 10.1016/j.vacuum.2021.110554

42. Singla AK, Banerjee M, Sharma A, *et al*. Selective laser melting of Ti6Al4V alloy: Process parameters, defects and post-treatments. *J Manuf Processes*. 2021;64:161-187.

doi: 10.1016/j.jmapro.2021.01.009

43. Zha S, Zhang H, Yang J, Zhang Z, Qi X, Zu Q. Fatigue threshold and microstructure characteristic of TC4 titanium alloy processed by laser shock. *Metals*. 2025;15(4):453.

doi: 10.3390/met15040453

44. Rodrigues RCS, Ribeiro RF, De Mattos MDC, Bezzon OL.

Comparative study of circumferential clasp retention force for titanium and cobalt-chromium removable partial dentures. *J Prosthet Dent*. 2002;88(3):290-296.

doi: 10.1067/mpr.2002.128128

45. Chastand V, Quaegebeur P, Maia W, Charkaluk E. Comparative study of fatigue properties of Ti-6Al-4V specimens built by electron beam melting (EBM) and selective laser melting (SLM). *Mater Charact*. 2018;143:76-81.

doi: 10.1016/j.matchar.2018.03.028

46. Parry L, Ashcroft IA, Wildman RD. Understanding the effect of laser scan strategy on residual stress in selective laser melting through thermo-mechanical simulation. *Addit Manuf*. 2016;12:1-15.

doi: 10.1016/j.addma.2016.05.014

47. Li C, Fu CH, Guo YB, Fang FZ. Fast prediction and validation of part distortion in selective laser melting. *Proced Manuf*. 2015;1:355-365.

doi: 10.1016/j.promfg.2015.09.042

48. Yang JJ, Yu HC, Yin J, Gao M, Wang ZM, Zeng XY. Formation and control of martensite in Ti-6Al-4V alloy produced by selective laser melting. *Mater Des*. 2016;108:308-318.

doi: 10.1016/j.matdes.2016.06.117

49. Kok Y, Tan XP, Wang P, *et al*. Anisotropy and heterogeneity of microstructure and mechanical properties in metal additive manufacturing: A critical review. *Mater Des*. 2017;139(FEB.):565-586.

doi: 10.1016/j.matdes.2017.11.021

50. Cao S, Chu RK, Zhou XG, *et al*. Role of martensite decomposition in tensile properties of selective laser melted Ti-6Al-4V. *J Alloy Compd*. 2018;744:357-363.

doi: 10.1016/j.jallcom.2018.02.111

51. Kruth JP, Deckers J, Yasa E, Wauthlé R. Assessing and comparing influencing factors of residual stresses in selective laser melting using a novel analysis method. *Proc Inst Mech Eng Part B J Eng Manuf*. 2012;226(B6):980-991.

doi: 10.1177/0954405412437085

52. Han SJ, Bang GB, Kim WR, *et al*. Effect on microstructural and mechanical properties of selective laser melted pure Ti parts using stress relief heat-treatment process. *J Mater Res Technol*. 2023;27:200-208.

doi: 10.1016/j.jmrt.2023.09.288

53. Yu WL, Zhu WL, Yin A, *et al*. Investigation of thermal stability of residual stresses and microstructure of dual shot peened TC17 titanium alloy. *J Alloy Compd*. 2025;1010:178075.

doi: 10.1016/j.jallcom.2024.178075

54. Li H, Jia D, Yang Z, *et al*. Effect of heat treatment on microstructure evolution and mechanical properties of selective laser melted Ti-6Al-4V and TiB/Ti-6Al-4V composite: A comparative study. *Mater Sci Eng A*. 2021;801:140415.

doi: 10.1016/j.msea.2020.140415

55. Chen SG, Ma JL, Gao HJ, Wang YS, Chen X. Research on residual stresses and microstructures of selective laser melted Ti6Al4V treated by thermal vibration stress relief. *Micromachines*. 2023;14(2):354.

doi: 10.3390/mi14020354

56. Skvortsova SV, Ivanov AE, Spektor VS, Shalin AV, Smirnov PA. Effect of heat treatment on the residual stresses, mechanical properties, and texture formation in VT6 alloy samples fabricated by selective laser melting. In: *Russian Metallurgy (Metally)*. Germany: Springer 2024;(2):2024.

doi: 10.1134/S0036029524700794

57. Tanaka A, Miyake N, Hotta H, Takemoto S, Yoshinari M, Yamashita S. Change in the retentive force of Akers clasp for zirconia crown by repetitive insertion and removal test. *J Prosthodont Res*. 2019;63(4):447-452.

doi: 10.1016/j.jpor.2019.02.005

58. Snyder HA, Duncanson MG Jr. The effect of clasp form on permanent deformation. *Int J Prosthodont*. 1992;5(4):345-350.

59. Bergman B, Hugoson A, Olsson CO. A 25 year longitudinal study of patients treated with removable partial dentures. *J Oral Rehabil*. 1995;22(8):595-599.

doi: 10.1111/j.1365-2842.1995.tb01055.x

60. Torii M, Nakata T, Takahashi K, Kawamura N, Shimpo H, Ohkubo C. Fitness and retentive force of cobalt-chromium alloy clasps fabricated with repeated laser sintering and milling. *J Prosthodont Res*. 2018;62(3):342-346.

doi: 10.1016/j.jpor.2018.01.001

61. Rues S, Tasaka A, Fleckenstein I, *et al*. Fit and retention of cobalt-chromium removable partial denture frameworks fabricated with selective laser melting. *J Funct Biomater*. 2023;14(7):416.

doi: 10.3390/jfb14080416

62. Ahmed N, Abbasi MS, Haider S, *et al*. Fit accuracy of removable partial denture frameworks fabricated with CAD/CAM, rapid prototyping, and conventional techniques: A systematic review. *Biomed Res Int*. 2021;2021:3194433.

doi: 10.1155/2021/3194433

63. Kola MZ, Raghav D, Kumar P, Alqahtani F, Murayshed MS, Bhagat TV. *In vitro* assessment of clasps of cobalt-chromium and nickel-titanium alloys in removable prosthesis. *J Contemp Dent Pract*. 2016;17(3):253-257.

doi: 10.5005/jp-journals-10024-1836

64. Ganor YI, Tiferet E, Vogel SC, *et al*. Tailoring microstructure and

mechanical properties of additively-manufactured Ti6Al4V using post processing. *Materials (Basel)*. 2021;14(3):658.

doi: 10.3390/ma14030658

65. Xu MR, Lin Y, Lin ZX, Cheng H. Elastic and fatigue properties of additively manufactured and milled Ti-6Al-4V removable partial denture clasps. *J Prosthet Dent*. 2025;133(1):230e1-230e8.

doi: 10.1016/j.prosdent.2024.09.017

66. Zhao ZY, Li L, Bai PK, *et al*. The heat treatment influence on the microstructure and hardness of TC4 titanium alloy manufactured via selective laser melting. *Materials (Basel)*. 2018;11(8):1318.

doi: 10.3390/ma11081318

67. Marie A, Keeling A, Hyde TP, *et al*. Deformation and retentive force following *in vitro* cyclic fatigue of cobalt-chrome and aryl ketone polymer (AKP) clasps. *Dent Mater*. 2019;35(6):E113-E121.

doi: 10.1016/j.dental.2019.02.028

68. Vallittu PK, Kokkonen M. Deflection fatigue of cobalt-chromium, titanium, and gold alloy cast denture clasp. *J Prosthet Dent*. 1995;74(4):412-419.

doi: 10.1016/s0022-3913(05)80384-1

69. Mahmoud A, Wakabayashi N, Takahashi H, Ohyama T. Deflection fatigue of Ti-6Al-7Nb, Co-Cr, and gold alloy cast clasps. *J Prosthet Dent*. 2005;93(2):183-188.

doi: 10.1016/j.prosdent.2004.11.011

70. Chen JB, She Y, Du XY, Liu YF, Yang Y, Yang JS. Influence of oxygen content on selective laser melting leading to the formation of spheroidization in additive manufacturing technology. *RSC Adv*. 2024;14(5):3202-3208.

doi: 10.1039/d3ra08627e

71. Barriobero-Vila P, Artzt K, Stark A, *et al*. Mapping the geometry of Ti-6Al-4V: From martensite decomposition to localized spheroidization during selective laser melting. *Scr Mater*. 2020;182:48-52.

doi: 10.1016/j.scriptamat.2020.02.043

72. Yin A, Yu WL, Li WB, *et al*. Microstructural and thermal relaxation of residual stress in dual peened TA15 titanium alloy fabricated by SLM. *Mater Charact*. 2024;218:114496.

doi: 10.1016/j.matchar.2024.114496